15th Triennial World Congress, Barcelona, Spain

# RADIOMETRIC IMAGE CORRECTION WITH AUTOMATIC MODEL SELECTION

**P. Carvalho, A. Santos, A. Dourado, B. Ribeiro** [1]

*Centre for Informatics and Systems, University of Coimbra*
*Pólo II, Pinhal de Marrocos, 3030 Coimbra, Portugal*
*Email: {carvalho, dourado, bribeiro}@dei.uc.pt*

Abstract: Computer vision is a powerful tool for intelligent sensor development. However, noise in CCD cameras leads to significant radiometric distortions. Therefore, radiometric image correction is a critical operation, specially when physics-based models are applied for image processing, as is the case in many industrial applications. All known radiometric correction methods assume that noise characteristics remain stable over time. In this paper, a new radiometric correction method is proposed to account for non static noise effects. The method decomposes radiometric distortion into multiplicative and additive errors, whose optimal models are computed with a new extension to the Generalized Cross-Validation Criterion.

Keywords: Precision Measurements, Model Selection, Cameras, Computer Vision.

## 1. INTRODUCTION

Image processing and pattern recognition techniques are powerful tools for building new intelligent sensors for industrial applications (see, for instance, (Batchelor and Whelan, 1997)). Most vision systems use CCD cameras for image acquisition. Their popularity stem from their linear response to light, ease of integration and low cost. Nevertheless, these devices are prone to several noise sources, which can induce significant radiometric distortions. Currently, there are two main streams of reasoning in image processing: (i) interpretation of an image as noise corrupted data, and (ii) using physical image formation models to interpret an image. Most of today's grey scale algorithms are inspired in the former approach. However, whenever exact information is to be inferred from images, the later approach is preferred, if not imperative. This is particularly true in color image processing, where precise image formation models are required to extract, for instance, reflection characteristics of materials (Farrell *et al.*, 1999). Other areas where this premise is important are 3D vision (Kamberova and Bajcsy, 1998) and image restoration applications (Kempen and Vliet, 1999), just to name a few.

Noise is an intrinsic property of the image formation process. Healey and Kondepudy (Healey and Kondepudy, 1994) have identified the main noise sources, which occur in the image formation process and have described an algorithm for the induced radiometric distortion correction. In their method, it is assumed that noise characteristics are static over time, i. e., their means and variances do not change. In practice, as will be shown, this behavior is only verified under very restricted conditions. For instance, the model assumes that dark current noise is stable. However, given its high temperature dependence, this assumption will only be verified if the temperature of the image acquisition environment is kept constant. Furthermore, the model assumes that the overall gain

[1] This project was partially financed by FCT/PRAXIS XXI (project 36564/99), and by POSI of the Portuguese Foundation for Science and Technology and the European Union FEDER. The project was performed at the Computacional Perception Laboratory at CISUC.

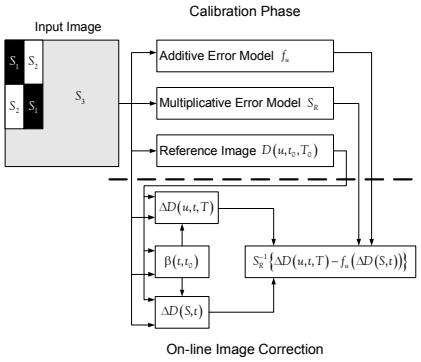


Fig. 1. Overview of the radiometric correction method.

of each image formation channel does not vary from image to image. Several authors (see (Chang and Reid, 1996) and references therein) have reported variations in channel gain, even when the automatic gain facility is turned off. Other methods have been proposed for radiometric image correction, which rely on the same premises. Kamberova and Bajcsy (Kamberova and Bajcsy, 1998) identify linear image transformations such that for an uniform surface, all pixels in the corrected image exhibit equal values.

All the above mentioned techniques rely on the camera's stable gain and noise characteristics over time. In this paper we propose a new radiometric correction procedure, which is able to estimate and correct the expected radiometric image distortion for variable gain and noise characteristics. Using an extended image formation model which accounts for changing noise characteristics with temperature, the proposed method operates as follows (see figure 1): (i) it is assumed that changes in radiometric distortion due to temperature can be described with multiplicative and additive error models, which are estimated during a calibration phase. (ii) Changes in additive and multiplicative errors with respect to a reference image are obtained from controlled regions in the image, either by placing reference surfaces in each image or by covering a small region of the CCD sensor, and from the computed error models. In this work, additive distortions between two regions of an image are modelled with regular polynomial functions. Some mild a priori knowledge on these mappings is applied to promote accuracy. Namely, it is seen that the required mappings must exhibit smoothness and monotonous behaviors. In this approach, to account for smoothness a regularization term is introduced in the criterion, being the trade-off between data fidelity and roughness controlled with a regularization gain. On the other hand, the monotonous behavior is accounted for by constraining the model's first order derivatives (see section 2). To select for proper model order and regularization gain, a new extended Generalized Cross Validation criterion ($GCV_{IC}$) is introduced (see section 3). In section 4 some results and main conclusions are presented.

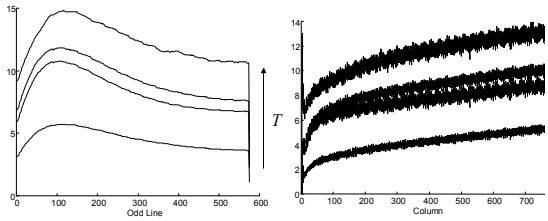


Fig. 2. Intensity variation of dark image obtained with a Sofretec CF 820 camera for distinct environment temperatures $T \in [6,20]^{\circ}\,C$. Left: average intensity for odd lines. Right: average intensity by column.

## 2. RADIOMETRIC IMAGE CORRECTION

Let $D(u,t,T)$ be the linearized camera output for point of coordinates $u \in \mathbb{N}^2$ at instant $t$ and temperature $T$, then

$$D(u,t,T) = \overline{D}(u,t,T) + N(u,t,T) \qquad (1)$$

where $N(u,t,T)$ is a random variable of mean zero and variance $\sigma_N^2(u,t,T)$ induced by shot, read and quantization noise and

$$\overline{D}(u,t,T) = A(t)\{S_R(u)\,I(u,t) + O(u,T)\} + N_F(u,t) \qquad (2)$$

$$O(u,T) \equiv N_D(u,T) + N_{FZ}(u) + N_{IL}(u,T)$$

In (2) $A(t)$, $S_R(u)$, $N_D(u,T)$, $N_{FZ}(u)$, $N_{IL}(u,T)$ and $N_F(u)$ represent, respectively, the channel gain, the photo response non uniformities (PRNU) in charge collection, the dark current charge (thermally induced charge), fat zero (artificial charge introduced by the readout circuitry to improve the sensor's spectral sensitivity $S(\lambda)$), internal luminance (mainly charge due to the clocking circuitry) and the offset introduced by the camera's transfer function for pixel $u$. $I(u,t)$ is defined as $\int_{\lambda_0}^{\lambda_n} I(\lambda,u,t)\,S(\lambda)\,d\lambda$, being $I(\lambda,u,t)$ the SPD (spectral power distribution) of the input radiation at point $u$ and instant $t$. For cameras with almost linear transfer functions, it can be shown that $E[N(u,t)] \to 0$, since it mainly describes the expectation of the zero mean sampling noise, and $\sigma_N^2$ is a linear function of $\overline{D}(u,t,T)$. In figure 2 several line and column statistics of dark images (images taken with the lens cap on) obtained under different environment temperatures with a Sofretec CF 820 CCD camera are shown. As can be observed, an environment temperature change of $14°C$ induces a variation in $N_D(u,T)$ and $N_{IL}(u,T)$ over 300% for this camera.

Let $R(\lambda,u,t)$ be the reflectance of a Lambertian planar surface, and let $I_E(\lambda)$ be the SPD of an

artificial light source projected onto that surface. From the dichromatic reflection model it follows that the light reflected from these surfaces can be modeled by the body reflection component, i. e.,

$$I(\lambda,u,t)=C_I(u)I_E(\lambda)R(\lambda,u,t) \tag{3}$$

where $C_I(u)\in[0,1]$ accounts for the geometrical dependent light power distribution and reflection attenuation. Before light interacts with a sensor's cell it has to travel through the lens system which introduces further attenuation and spectral transformation. Let $L(\lambda)$ be the spectral transmittance from the target to the CCD and $C_L(u)$ be the lens light attenuation effect (such as the $cos^4$ and the vignetting effects), then $(C_{LI}(u)=C_I(u)C_L(u))$

$$I(\lambda,u,t)=C_{LI}(u)I_E(\lambda)R(\lambda,u,t)L(\lambda) \tag{4}$$

Hence, to perform radiometric image correction, for each image the multiplicative errors $S_R(u)$ and $A(t)$, and the additive error $A(t)O(u,T)$ $+N_F(u,t)$ have to be estimated. Instead of computing the absolute values for the camera's gain and offset error, in this correction approach relative values, with respect to a reference image $D(u,t_0,T_0)$, $\beta(t,t_0)=A(t_0)/A(t)$ and $\Delta D(u,t)=A(t_0)\{O(u,T)-O(u,T_0)\}$ are identified. This enables correction results given by $\tilde{D}(u)=A(t_0)C_{LI}(u)\int_{\lambda_0}^{\lambda_n}I_E(\lambda)R(\lambda,u,t)L(\lambda)d\lambda$.

Let us assume that each image is composed by three different regions $S_i$, $i=1,..,3$, such that $S_1$ and $S_2$ form a chess pattern as shown in figure 1. Further, let us assume that no changes in $I(\lambda,u,t)$ occur, i. e., the illumination $I_E(\lambda)$ and the reflectance characteristics $R(\lambda,u,t)$, $u\in\{S_1,S_2\}$, are kept constant over time. The relative changes in additive error $\Delta D(u,t)$ and multiplicative error $\beta(t,t_0)$ can be computed from the image regions $S_1$ and $S_2$. Notice that under general computer vision conditions these constraints may not be feasible. In these cases, $\Delta D(u,t)$ can still be computed by covering region $S_1$ and $S_2$ of the CCD sensor such that no photocurrent is generated for these sensor cells. However, under these circumstances, the method is unable to estimate $\beta(t,t_0)$. As long as automatic gain is turned off, as will be shown, good correction results can still be achieved.

Let $D(S_i,t,T)$ be the average image intensity in region $S_i$, i. e., $D(S_i,t,T)=(s(t)\|S_i\|)^{-1}\sum_{u\in S_i}$ $\sum_{t_w\in s(t)}D(u,t_w,T_w)$, where $s(t)$ and $\|S_i\|$ are respectively the number of images taken and the number of pixels in region $S_i$, and let $D(u,t_0,T_0)$ be a reference image. Evaluating the difference between mean intensities in regions $S_1$ and $S_2$, it is seen that $(I_i=I(u,t)\equiv\int I(\lambda,u,t)S(\lambda)d\lambda$, $u\in S_i$, $i=1,2)$,

$$\begin{aligned}Z(S_1,S_2,t,T)&=D(S_2,t,T)-D(S_1,t,T)\\&=\frac{A(t)}{s(t)\|S_i\|}\left\{I_2\sum_{u\in S2}C_{LI}(u)S_R(u)-\right.\\&\left.-I_1\sum_{u\in S1}C_{LI}(u)S_R(u)\right\}+\Delta N(S_2,S_1)\end{aligned} \tag{5}$$

In practice, given that both regions $S_1$ and $S_2$ share the same columns and lines of the image, it is observed that $\Delta N(S_2,S_1)\to 0$. Hence, as long $I_1\ll I_2$, it is seen that (5) enables the estimation of $\beta(t,t_0)$. Namely,

$$\beta(t,t_0)\equiv\frac{Z(S_1,S_2,t_0,T_0)}{Z(S_1,S_2,t,T)} \tag{6}$$

If $\|S_1\|=\|S_2\|$ and $s(t_0)$ is taken large enough such that the uncertainty in (6) is mainly conditioned by the data at instant $t$, it can be shown that the expected value for $\beta(t,t_0)$, $E[\beta(t,t_0)]$, and its variance $V[\beta(t,t_0)]$ can be computed as in (7) and (8), where $\sigma^2_{S_i}(t)=(s(t)\|S_i\|)^{-1}\sum_{u\in S_i}$ $\sum_{t_w\in s(t)}\sigma^2_N(u,t_w,T_w)$ is the average noise variance in region $S_i, i=1,2$.

$$E[\beta(t,t_0)]\simeq A(t)^{-1}A(t_0) \tag{7}$$

$$V[\beta(t,t_0)]\simeq\frac{\left(\sigma^2_{S_1}(t)+\sigma^2_{S_2}(t)\right)E[Z(S_1,S_2,t,T_0)]^2}{s(t)\|S_1\|E[Z(S_1,S_2,t,T)]^4} \tag{8}$$

On the other hand, the change in the additive error in region $S_1$ can be computed from $\Delta D(S_1,t)=\beta(t,t_0)^{-1}D(S_1,t,T)-D(S_1,t_0,T_0)$, which leads to

$$E[\Delta D(S_1,t)]=A(t_0)\{O(S_1,T)-O(S_1,T_0)\} \tag{9}$$

$$\begin{aligned}V[\Delta D(S_1,t)]\simeq\sigma^2_{S_1}(t)E[\beta(t,t_0)]^2+\\+V[\beta(t,t_0)]E[D(S_1,t,T)]^2\end{aligned} \tag{10}$$

From (8) and (10), it is concluded that, in order to minimize the uncertainty of these estimates, the reference surfaces for $S_1$ should be chosen such that $R(\lambda,u,t)\to 0$, $u\in S_1$, and $R(\lambda,u,t)\to 1$, $u\in S_2$, i.e., a black and a white reference surface, respectively. Taking a similar approach for the image in region $S_3$, it is observed that $\Delta D(u,t)\equiv$ $\beta(t,t_0)^{-1}D(u,t,T)-D(u,t_0,T_0)$. Hence,

$$\begin{aligned}\Delta D(u,t)=A(t_0)S_R(u)I(u,t)+\\+A(t_0)(O(u,T)-O(u,T_0))\end{aligned} \tag{11}$$

Note that in (11) it is assumed that $I(u,t_0)=0$, $u\in S_3$, while in (7) and (9) it is considered that $I(u,t_0)\neq 0$, $u\in\{S_1,S_2\}$. This can be accomplished if the reference image is computed from two distinct images taken with the same sensor temperature: from the first image, obtained with the sensor exposed to light, the data for $D(u,t_0,T_0)$, $u\in\{S_1,S_2\}$, are taken, while from

the second image, obtained with the lens cap one, pixels $D(u,t_0,T_0)$ from region $S_3$ are estimated. To avoid distinct gains $A(t)$ for the two images, these should be computed from an average of a large sequence of images acquired with automatic gain disabled.

Equations (9) and (11) are the basis of the correction method. Namely, if the mapping $y = f_u(a)$, $y \equiv A(t_0)(O(u,T) - O(u,T_0))$, $u \in S_3$, $a \equiv A(t_0)(O(S_1,T) - O(S_1,T_0))$, are known, then an image without bias can be obtained from $\Delta D(u,t) - f_u(A(t_0)(O(S_1,T) - O(S_1,T_0)))$. Since the physical laws which describe these mappings are not known, a generic formulation is applied to identify $f_u$, i.e., $f_u(a) = \sum_{i=0}^{n} x_i X_i(a)$, $n \in \mathbb{N}$, $x_i \in \mathbb{R}$, where $X_i$ can be any basis function. There are some a priori knowledge that can be integrated into the estimation process to enable a better estimation accuracy: (i) it is seen that $f_u$ is monotonous increasing, although not linear for large variation in temperature. The monotonous behavior is mainly due to blackcurrent. This charge follows a Boltzmann distribution, hence increases with temperature. Nonlinearity, is due to blackcurrent and due to internal illuminance generated charge. (ii) Further, $f_u$ should be smooth. In the proposed estimation technique, smoothness is imposed by a regularization term in the criterion build upon the second derivative of $f_u$, being the trade-off between data accuracy and smoothness controlled with a positive regularization gain, i.e., $\lambda \in \mathbb{R}^+$. For smoothness measure the second derivative of $f_u$ is applied. As for the monotonous behavior of the function, it can be obtained by constraining the first derivative of the function to be positive or zero at $k$ regular points. Hence, if a set of calibration points $\{(y_i, a_i) : i = 1, ..., m\}$ are known for distinct temperatures (obtained from black images with AGC turned off), $f_u$ can be identified by formalizing the estimation problem in terms of a quadratic criterion minimization subject to linear inequality constraints as in (12) ($A \equiv \left[A_1^T, ..., A_m^T\right]^T \in \mathbb{R}^{m \times n}$, $A_i \equiv [X_1(a_i), ..., X_n(a_i)]$, $i = 1, ..., m$, $b \equiv [y_1, ..., y_m]^T$, $D \in \mathbb{R}^{n-2 \times n}$, $C \in \mathbb{R}^{k \times n}$, $x = [x_1, ..., x_n]^T$). Note that $C$ and $D$ encode $-df_u/da$ and $d^2 f_u/da^2$, respectively.

$$\min_x \left\{ \|Ax - b\|^2 + \lambda \|Dx\|^2 \right\} : Cx \leq 0 \qquad (12)$$

Given $n$ and $\lambda$, the best solution can be computed from (12). However, the optimal $n$ and $\lambda$ are not known. If $n$ is chosen too small, then $f_u$ will not be able to capture the dynamics of the data, while choosing $n$ too high will induce overfitting and probably some oscillation. On the other hand if $\lambda \to \infty$, then (12) will identify a line, while, if $\lambda \to 0$ then, again, oscillation may occur. Given the enormous amount of data and given that $n$ and $\lambda$ are not global to the image, an automatic strategy for selecting $n$ and $\lambda$ is required. This is a typical problem of model selection. There are several model selection techniques (for a survey see (Hansen and Yu, 2001)). In this work an extended Generalized Cross-Validation Criterion ($GCV_{IC}$) is applied. Namely, select $\widehat{x}$, $n$ and $\lambda$ such that $\min_{n,\lambda} \{GCV_{IC}(n,\lambda)\}$ (as defined in (19)). Finally, to compensate for PRNU noise, a similar approach as in (Healey and Kondepudy, 1994) is followed and, therefore, the corrected image can be computed as described in (13).

$$\widetilde{D}(u) = S_R^{-1}(u)(\Delta D(u,t) - f_u(\Delta D(S_1,t))) \qquad (13)$$

## 3. THE EXTENDED GCV MEASURE

The idea of the $GCV_{IC}$ is to test how well the estimated model predicts data for different roughness penalty values $\lambda$ and model orders $n$. This idea was first applied by Craven and Wahba (Craven and Wahba, 1979) and led to the introduction of the $GCV$ (generalized cross-validation) measure for the unconstrained fitting problem. In this work, the $GCV$ is extended to the linear inequality constrained fitting problem. This extension results in a new $GCV$ measure, the $GCV_{IC}$. The fitting problem can be written as in (14).

$$\min_x \left\{ \|A^* x - b^*\|^2 \right\} : Cx \leq H \qquad (14)$$

$$A^* = \begin{bmatrix} A \\ \sqrt{\lambda} D \end{bmatrix}, b^* = \begin{bmatrix} b \\ 0 \end{bmatrix} \qquad (15)$$

From the active set theory (Ciarlet and Lions, 1990) it is known that the solution to the problem in (14) is equivalent to solve an equality constrained problem with the subset of constraints which, for a particular solution, are active. Let $C^* \widehat{x} = H^*$, $C^* \subseteq C$, $C^* \in \mathbb{R}^{h \times n}$, $h \leq k$, be the subset of constraints in (14) verified with equality, then the solution can be found using the following corollary:

*Corollary 1.* Let $\widehat{x}(\lambda, n)$ be the solution to (14). Then, if $C^* \widehat{x}(\lambda, n) = 0$ are the subset of active constraints, $\widehat{x}$ verifies

$$\widehat{x}(\lambda, n) = \Omega(\lambda, n) + \Theta(\lambda, n) b \qquad (16)$$

with $\Omega(\lambda, n) = Z_1 \widetilde{D}_C^{-1} W_C^T H^*$, $\Theta(\lambda, n) = Z_2 \widetilde{D}_A^{-1} W_{21}$, $Z^{-1} = \begin{bmatrix} \underbrace{Z_1}_{p} & \underbrace{Z_2}_{n-p} \end{bmatrix}$, $A^* = W_A \begin{bmatrix} D_A^T & 0 \end{bmatrix}^T Z$, $C^* = W_C \begin{bmatrix} D_C & 0 \end{bmatrix} Z$ are the generalized singular value decompositions of $A^*$ and $C^*$, $D_A = diag(\alpha_1, ..., \alpha_n)$, $D_C = diag(\beta_1, ..., \beta_p, 0)$, $\widetilde{D}_A = diag(\alpha_{p+1}, ..., \alpha_n)$, $\widetilde{D}_C = diag(\beta_1, ..., \beta_p)$ and

$$W_A^T = \begin{bmatrix} \overbrace{W_{11}}^{m} & \overbrace{W_{12}}^{v} \\ W_{21} & W_{22} \\ W_{31} & W_{32} \end{bmatrix} \begin{matrix} p \\ n-p \\ m+v-n \end{matrix}$$

(Proof is immediate by taking theorem 1 and the formulation in (14) and some simple algebraic manipulations.)

Let $\widehat{x}^{[k]}(n,\lambda)$ denote the estimate of $x$ using all but the $k$th data point of $b$. The $OCV$ (Ordinary Cross-Validation) function measures the overall predictability of data points by the estimate $\widehat{x}^{[k]}(n,\lambda)$ and is defined by ($b_k$ - $k$th element of vector $b$; $A_k$ - $k$th row vector of matrix $A$)

$$OCV(\lambda,n) = \frac{1}{m}\sum_{k=1}^{m}\left(b_k - A_k\widehat{x}^{[k]}(\lambda,n)\right)^2 \quad (17)$$

To derive the $GCV_{IC}(\lambda,n)$ function from (17) some theorems have to be introduced.

*Lemma 2.* Let $h(k,z)$ be the solution to (14) with linear equality constraints and with the $k$th data point replaced by $z$, then $h(k, A_k\widehat{x}^{[k]}(\lambda,n)) = \widehat{x}^{[k]}(\lambda,n)$. (Proof is immediate)

*Theorem 3.* The $OCV_{IC}(\lambda,n)$ function for the problem defined in (14) with linear equality constraints is

$$OCV_{IC}(\lambda,n) = \frac{1}{m}\sum_{k=1}^{m}\frac{\left(b_k - A_k\widehat{x}(\lambda,n)\right)^2}{(1-\rho_{kk})^2} \quad (18)$$

where $\rho_{kk}$ is the $kk$th element of $A\Theta(\lambda,n)$ and $\Theta(\lambda,n)$ is as defined in (16) .

**Proof.** Taking Lemma 2, it is straightforward to proof that

$$b_k - A_k\widehat{x}(\lambda,n) = (1-\rho_{kk})\left(b_k - A_k\widehat{x}^{[k]}(\lambda,n)\right)$$

■

*Theorem 4.* The $GCV_{IC}(\lambda,n)$ function for the problem defined in (14) is

$$GCV_{IC}(\lambda,n) = \frac{\frac{1}{m}\left\|b - A\widehat{x}(\lambda,n)\right\|^2}{\left(\frac{1}{m}trace\,(I-\rho)\right)^2} \quad (19)$$

**Proof.**

To proof this result a weighted $OCV_{IC}$ is taken to account for non equally spaced data points, as suggested in (Craven and Wahba, 1979). It can be shown that $\rho$ is symmetric. Hence, there exists a transformation matrix $\Gamma$ such that $\Gamma\rho\Gamma^T$ is circulant. Taking $OCV_{IC}$ on this new system, it follows that the data points are equally spaced and the transformation is equivalent to take a weighted $OCV_{IC}$ with weights $w_k = \left[(1-\rho_{kk})/trace(I-\rho)\right]^2$. Hence, substituting this in (18), (19) is verified. ■

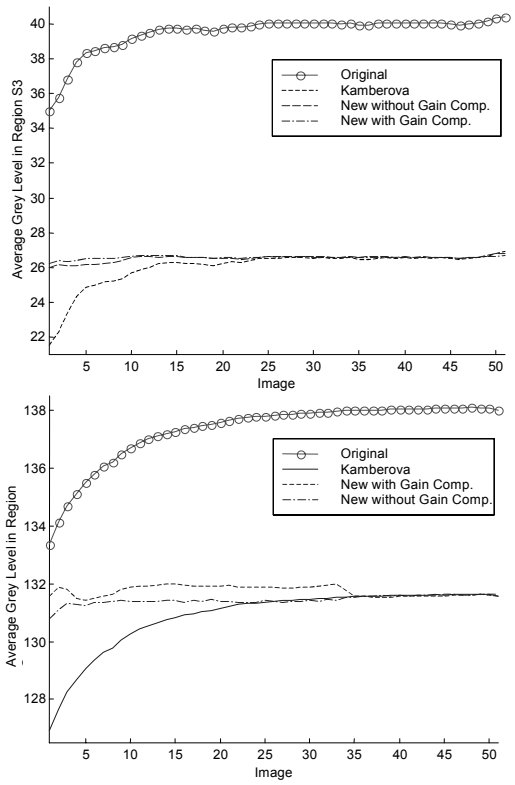


Fig. 3. Comparison of radiometric correction results of two sequences of images taken during the heat up of a Sofretec CF820 camera. Both image sequences were captured from patches of the MacBeth ColorChecker map using different illumination setups . (Top) Image sequence 1 - dark grey patch. (Bottom) Image sequence 2 - grey patch. The values shown correspond to the average grey level of pixels in region $S_3$.

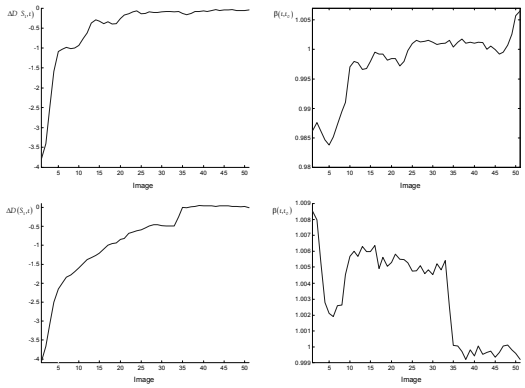

Fig. 4. Variation of $\Delta D\,(S_1,t)$ and of $\beta\,(t,t_0)$. (Top) Image sequence 1. (Bottom) Image sequence 2.

## 4. RESULTS AND CONCLUSIONS

In figure (3) a comparison between Kamberova's flatfielding algorithm and the introduced method is shown. These results were obtained from two sequences of 51 images taken with a Sofretc CF820

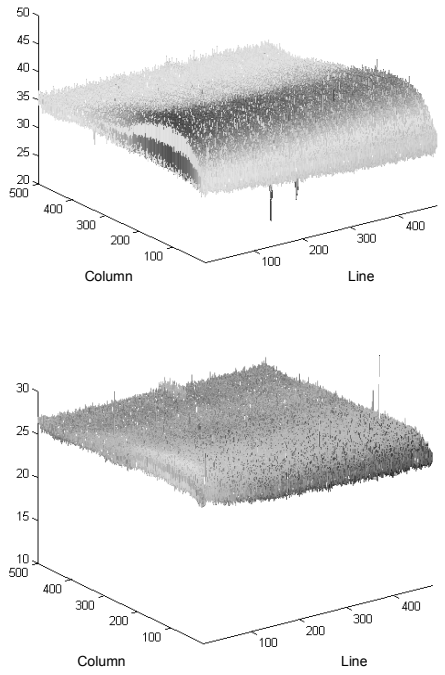


Fig. 5. Correction results for image no. 1 of image sequence no. 1. (Top) Original image (Bottom) Correction result with new method with gain compensation.

CCD camera for the dark grey patch of the MacBeth ColorChecker and for its grey patch using different illumination setups. In each image sequence the ambient temperature was varied from about $0°C$ to around $22°C$. Further, the reference image was computed at $T \simeq 22°C$. The results presented are the average grey level in region $S_3$. The additive error model orders were computed using the described $GCV_{IC}$ criterion, which lead to an average model order of 4.43. In figure (5) the first image of the grey patch sequence is depict. As can be observed, all pixels' additive error models were properly captured with this strategy. The use of $GCV_{IC}$ is an important aspect, since besides avoiding over or underfitting, which could occur by arbitrating a global model order and regularization gain, it optimizes memory requirements for model coefficients storage.

For the dark grey patch image sequence, it is seen that the uncorrected image sequence exhibits an average grey value variation of 5.3688 and a pixel grey level standard deviation between 2.2530 and 2.4367. As temperature changes, static correction strategies are unable to compensate for changing noise characteristics. Namely, using Kamberova's flatfielding techniques, it is seen that the average grey value variation is similar (5.3498) to the one observed for the uncorrected image sequence, although the grey level standard deviation is drastically reduced in this case (between 0.5348 and 0.9661). This is as due to PRNU as due to black current correction. On the other hand, the application of the algorithm described in section 2 enables a drastic reduction of the average bias (0.4746 for the algorithm with gain compensation, and 0.8270 if gain compensation is disabled). As for the pixels' standard deviation, intervals $[0.5396, 0.7906]$ and $[0.5393, 0.8001]$ are respectively obtained for the algorithm with and without gain compensation. Similar results are also obtained for the grey patch image sequence (see figure 3 bottom). As expected, for $T$ around $22°C$, the algorithm performs as Kamberova's method, since in these circumstances the expected noise characteristics are similar in both methods. These results suggest that the described algorithm is applicable both in industrial applications of CCD sensors, where usually illumination control and the positioning of the required reference surfaces for gain compensation are feasible, and general computer vision tasks, where these conditions are usually not practical or even impossible to implement.

## 5. REFERENCES

Batchelor, B. and P. Whelan (1997). *Intelligent Vision Systems for Industry.*

Chang, Y.-C. and J. F. Reid (1996). RGB calibration for color image analysis in machine vision. *IEEE Trans. on Image Processing* **5**(19), 1414–1422.

Ciarlet, P. and J. Lions (1990). *Handbook of Numerical Analysis.* Elsevier-North Holland.

Craven, P. and G. Wahba (1979). Smoothing noisy data with spline functions. *Numer. Math.* **31**(1), 377–403.

Farrell, J., J. Cupitt, D. Saunders and B. Wandell (1999). Estimating spectral reflectances of digital artwork. In: *Chiba Confernce on Multispectral Imaging.*

Hansen, M. and B. Yu (2001). Model selection and the principle of minimum description length. *JASA* **96**(454), 746–774.

Healey, G. E. and R. Kondepudy (1994). Radiometric CCD camera calibration and noise estimation. *IEEE Trans. on Pattern Anal. Machine Intell.* **16**(3), 267–276.

Kamberova, G. and R. Bajcsy (1998). Sensor errors and the uncertainties in stereo reconstruction. In: *Proc. IEEE Workshop on Empirical Evaluation Techniques in Computer Vision.*

Kempen, G. and L. Vliet (1999). The influence of the background estimation on the superresolution properties of non-linear image restoration algorithms. In: *Proc. of the Three Dimensional and Multi-Dimensional Microscopy: Image Acquisition and Processing.* pp. 179–189.